CHEMISTRY OF MATERIALS
Article

Chem. Mater. **2011,** *23,* 239–246 239
DOI:10.1021/cm103426w

Phenolic Polyene Crystals with Tailored Physical Properties and Very Large Nonlinear Optical Response

O-Pil Kwon,*,† Seong-Ji Kwon,‡ Mojca Jazbinsek,*,‡ Ji-Youn Seo,† Jong-Taek Kim,§ Jung-In Seo,§ Yoon Sup Lee,§ Hoseop Yun,⊥ and Peter Günter‡

†*Department of Molecular Science and Technology, Ajou University, Suwon 443-749, Korea,* ‡*Nonlinear Optics Laboratory, ETH Zurich, CH-8093 Zurich, Switzerland,* §*Department of Chemistry and School of Molecular Science (BK 21), Korea Advanced Institute of Science and Technology (KAIST), Daejeon 305-701, Korea, and* ⊥*Division of Energy Systems Research and Department of Chemistry, Ajou University, Suwon 443-749, Korea*

Received October 4, 2010

We report on the design of the nonlinear optical organic phenolic polyene crystals for tailoring their physical properties to achieve optimized crystals for applications. New phenolic OH2 (2-(3-(4-hydroxystyryl)-5-methylcyclohex-2-enylidene)malononitrile) molecules keep the main supramolecular interaction sites and the high hyperpolarizability of the previously studied state-of-the-art OH1 (2-(3-(4-hydroxystyryl)-5,5-dimethylcyclohex-2-enylidene)malononitrile) and OH3 (2-(3-(4-hydroxystyryl)cyclohex-2-enylidene)malononitrile) molecules but contain different substituents in the non-π-conjugated part of the molecule, which affects the crystal packing and the physical properties. The acentric OH2 crystals exhibit an improved molecular ordering compared to OH1 crystals, leading to a high order parameter $\cos^3 \theta_p = 0.92$, which is close to optimal for electro-optics and terahertz generation applications. They also exhibit a considerably improved solution growth characteristics compared to the isomorphous OH3 crystals, based on the increase of the solubility by a factor of 2. The acentric OH2 crystals exhibit a large macroscopic nonlinearity with up to twice the second harmonic generation efficiency of OH1 and OH3 crystals as well as the possibility to grow bulk crystals suitable for optical investigations. Furthermore, we evaluate theoretically that the head-to-tail intermolecular hydrogen bonds occurring in phenolic polyene crystals may enhance the hyperpolarizability of the molecules by 50% or more.

Introduction

Organic molecular crystals, having three-dimensional spatial ordering of constituent molecules in contrast to amorphous materials having only short-range molecular ordering, are very attractive in numerous areas from fundamental science to industrial applications.[1−3] To obtain desired physical properties by crystal engineering, the molecular design is most challenging due to the tendency of imperfect molecular ordering in the crystalline state.[4] In many cases, a small variation of the chemical structure of the constituent molecules is accompanied with a large change of molecular ordering in the crystalline state and may lead to a substantial change of the macroscopic physical properties.[5,6] This is crucial for second-order nonlinear optical materials[7] interesting for integrated photonics[8] and terahertz wave applications,[9] which require acentric molecular ordering in bulk materials. For these applications, most often a high diagonal nonlinear optical susceptibility element is required, for which the optimal crystal structure is the one with the perfectly parallel

*To whom correspondence should be addressed. E-mail: opilkwon@ajou.ac.kr (O.-P.K.), nlo@phys.ethz.ch (M.J.).

(1) (a) Schwoerer, M.; Wolf, H. C. In *Organic Molecular Solids*; Wiley-VCH: Weinheim, 2007. (b) Tung, H. H.; Paul, E. L.; Midler, M.; McCauley, J. A. In *Crystallization of Organic Compounds: An Industrial Perspective*; Wiley: NJ, 2009.
(2) (a) *Introduction to Organic Electronic and Optoelectronic Materials and Devices*; Sun, S. S., Dalton, L. R., Eds.; CRC Press: Boca Raton, FL, 2008. (b) Braga, D.; Horowiz, G. *Adv. Mater.* **2009**, *21*, 1473. (c) *Organic Electronics* (special issue), J. Mater. Res. **2004**, *19*, 1887-2099.
(3) (a) Zhao, Y. S.; Fu, H.; Peng, A.; Ma, Y.; Xiao, D.; Yao, J. **2008**, *20*, 2859. (b) Patra, A.; Anthony, S. P.; Radhakrishnan, T. P. *Adv. Funct. Mater.* **2007**, *17*, 2077. (c) Sanz, N.; Wang, I.; Zaccaro, J.; Beaugnon, E.; Baldeck, P. L.; Ibannez, A. *Adv. Funct. Mater.* **2002**, *12*, 352.
(4) (a) Aakeroy, C. B. *Acta Crystallogr., Sect. B: Struct. Sci.* **1997**, *B53*, 569. (b) Aakeroy, C. B.; Seddon, K. R. *Chem. Soc. Rev.* **1993**, 397. (c) Sharma, C. V. K. *Cryst. Growth Des.* **2002**, *2*, 465.
(5) Desiraju, G. R. *Angew. Chem., Int. Ed.* **2007**, *46*, 8342.
(6) Braga, D.; Brammer, L.; Champness, N. R. *CrystEngComm* **2005**, *7*, 1.
(7) (a) Nalwa, H. S.; Watanabe, T. Miyata, S. In *Nonlinear Optics of Organic Molecules and Polymers*; Nalwa, H. S., Miyata, S., Eds.; CRC Press: 1997; Ch. 4. (b) Bosshard, Ch.; Bösch, M.; Liakatas, I.; Jäger, M.; Günter, P. In *Nonlinear Optical Effects and Materials*; Günter, P., Ed.; Springer-Verlag: Berlin, 2000; Ch. 3. (c) Chemla, D. S.; Zyss, J. J. in *Nonlinear Optical Properties of Organic Molecules and Crystals*; Academic Press: 1987; Vol. *1*.
(8) (a) Jazbinsek, M.; Kwon, O. P.; Bosshard, Ch.; Günter, P. In *Handbook of Organic Electronics and Photonics*; Nalwa, S. H., Ed.; American Scientific Publishers: Los Angeles, 2008; Ch. 1. (b) Ma, H.; Jen, A. K. Y.; Dalton, L. R. *Adv. Mater.* **2002**, *14*, 1339. (c) Dalton, L. R.; Sullivan, P. A. *Chem. Rev.* **2010**, *110*, 25.
(9) (a) Tonouchi, M. *Nat. Photonics* **2007**, *1*, 97. (b) Ferguson, B.; Zhang, X. C. *Nat. Mater.* **2002**, *1*, 26. (c) Hashimoto, H.; Takahashi, H.; Yamada, T.; Kuroyanagi, K.; Kobayashi, T. *J. Phys.: Condens. Matter.* **2001**, *13*, L529. (d) Matsukawa, T.; Mineno, Y.; Odani, T.; Okada, S.; Taniuchi, T.; Nakanishi, H. *J. Cryst. Growth* **2007**, *299*, 344.

Published on Web 12/27/2010

chromophore orientation. Therefore, up to now only a few organic crystals exhibiting large macroscopic optical nonlinearity have been developed.[10−15] These include the widely investigated ionic stilbazolium salts based on Coulomb interactions[10,11] and the recently developed configurationally locked polyene (CLP) crystals based on hydrogen bonds.[13−15] The state-of-the-art organic nonlinear optical crystals are the organic salts DAST (*N,N*-dimethylamino-*N*′-methylstilbazolium 4-methylbenzenesulfonate),[10] DSTMS (*N,N*-dimethylamino-*N*′-methylstilbazolium 2,4,6-trimethylbenzenesulfonate),[11a] and other stilbazolium salts[11] as well as the hydrogen-bonded CLP crystal OH1 (2-(3-(4-hydroxystyryl)-5,5-dimethylcyclohex-2-enylidene)malononitrile),[15] which are the only commercially available nonlinear organic crystals[16] with very large nonresonant nonlinear optical susceptibility $\chi^{(2)}_{iii}(-2\omega,\omega,\omega) > 240$ pm/V at 1.9 μm and large electro-optic coefficient $r_{iii} > 50$ pm/V at 1.3 μm.[17] These crystals also exhibit best figures of merit for THz generation by optical rectification or difference frequency generation, which is because of their high diagonal $\chi^{(2)}$ susceptibility element as well as a low dielectric dispersion important for the phase matching between the pump optical and the generated THz waves.[17a,18,19] For the same reason and the possibility for phase matching between optical and electric signals, these crystals are also very suitable for highly efficient and ultrafast electro-optics with bandwidths beyond 40 GHz.[17a]

For practical applications, not only a large macroscopic nonlinearity with optimal molecular ordering is required but also other crystal characteristics including crystal growth, solubility,[11a] thermal properties[13a] including the melting point and the thermal stability are important. However, due to the challenging design of highly nonlinear optical molecules exhibiting a desired acentric molecular orientation in the crystalline state, there are only few successful systematic studies of the molecular design to achieve tailored physical properties.

Here we report on the rational design of organic phenolic configurationally locked polyene (CLP) crystals for tailoring their physical properties. Previously studied phenolic CLP crystals exhibit partially nonoptimal physical properties. OH1 crystals exhibit an excellent crystal growth and good but not optimal molecular ordering with the order parameter of $\cos^3(\theta_p) = 0.69$, where θ_p is the angle between the charge transfer axis of the chromophores and the polar axis of the crystal.[15,20] On the other hand, the derivative OH3 crystals (2-(3-(4-hydroxystyryl)cyclohex-2-enylidene)malononitrile) exhibit molecular ordering with an almost perfect order parameter of $\cos^3(\theta_p) = 0.93$ but poor crystal growth due to the low solubility.[21] We have designed new phenolic CLP crystals containing different substituents in the non-π-conjugated part in the cyclohexene ring for maintaining the main supramolecular interactions existing in OH1 and OH3 but modifying the molecular ordering and other physical properties. The microscopic and macroscopic nonlinearities of the CLP crystals are investigated experimentally and theoretically. New OH2 (2-(3-(4-hydroxystyryl)-5-methylcyclohex-2-enylidene)malononitrile) crystals with two polymorphic forms have been obtained, with the acentric monoclinic space-group symmetry *Cc* (OH2-(I)) and centrosymmetric monoclinic space-group symmetry $P2_1/n$ (OH2-(II)). OH2-(I) crystals exhibit a very large macroscopic nonlinearity with up to twice the second harmonic generation efficiency of OH1 crystals, which is attributed to optimal molecular alignment with a high order parameter $\cos^3\theta_p = 0.92$. Moreover, OH2 crystals in contrast to OH3 crystals show a good crystal growth with about twice the solubility in methanol, and therefore OH2 bulk crystals suitable for optical investigations could be successfully grown.

Experimental Section

Synthesis. The phenolic OH2 chromophore was synthesized by Knoevenagel condensations with 4-hydroxybenzaldehyde and the intermediate 2-(3,5-dimethylcyclohex-2-enylidene)malononitrile according to the literature.[15,22] The materials were purified by recrystallization in methanol and ethylacetate.

OH2 (*2-(3-(4-Hydroxystyryl)-5-methylcyclohex-2-enylidene)-malononitrile*). ^{1}H NMR (CD_3OD, δ): 1.07 (3H, s, $-CH_3$), 2.2−2.4 (3H, $-CH_2-$, $-CH-$), 2.8−3.0 (2H, m, $-CH_2-$), 6.76 (1H, s, -*C* = CH−), 6.78−6.81 (2H, d, $J = 8.7$ Hz, Ar−H), 6.94−6.99 (1H, d, $J = 18$ Hz, −CH=CH-), 7.16−7.22 (1H, d,

(10) (a) Marder, S. R.; Perry, J. W.; Schaefer, W. P. *Science* **1989**, *245*, 626. (b) Marder, S. R.; Perry, J. W.; Yakymyshyn, C. P. *Chem. Mater.* **1994**, *6*, 1137. (c) Pan, F.; Wong, M. S.; Bosshard, Ch.; Günter, P. *Adv. Mater.* **1996**, *8*, 592.
(11) (a) Yang, Z.; Mutter, L.; Stillhart, M.; Ruiz, B.; Aravazhi, S.; Jazbinsek, M.; Schneider, A.; Gramlich, V.; Günter, P. *Adv. Funct. Mater.* **2007**, *17*, 2018. (b) Yang, Z.; Jazbinsek, M.; Ruiz, B.; Aravazhi, S.; Gramlich, V.; Günter, P. *Chem. Mater.* **2007**, *19*, 3512. (c) Ogawa, J.; Okada, S.; Glavcheva, Z.; Nakanishi, H. *J. Cryst. Growth* **2008**, *310*, 836. (d) Coe, B. J.; Harris, J. A.; Asselberghs, I.; Wostyn, K.; Clays, K.; Persoons, A.; Brunschwig, B. S.; Coles, S. J.; Gelbrich, T.; Light, M. E.; Hursthouse, M. B.; Nakatani, K. *Adv. Funct. Mater.* **2003**, *13*, 347.
(12) (a) Serbutoviez, Ch.; Bosshard, Ch.; Knopfle, G.; Wyss, P.; Pretre, P.; Günter, P.; Schenk, K.; Solari, E.; Chapuis, G. *Chem. Mater.* **1995**, *7*, 1198. (b) Zyss, J.; Nocoud, J. F.; Coquillay, M. *J. Chem. Phys.* **1984**, *81*, 4160.
(13) (a) Kwon, O. P.; Ruiz, B.; Choubey, A.; Mutter, L.; Schneider, A.; Jazbinsek, M.; Günter, P. *Chem. Mater.* **2006**, *18*, 4049. (b) Khan, R.; Kwon, O. P.; Tapponnier, A.; Rashid, A.; Günter, P. *Adv. Funct. Mater.* **2006**, *16*, 180. (c) Kwon, S. J.; Kwon, O. P.; Jazbinsek, M.; Gramlich, V.; Günter, P. *Chem. Commun.* **2006**, 3729.
(14) Kwon, O. P.; Kwon, S. J.; Jazbinsek, M.; Gramlich, V.; Günter, P. *Adv. Funct. Mater.* **2007**, *17*, 1750.
(15) Kwon, O. P.; Kwon, S. J.; Jazbinsek, M.; Brunner, F. D.; J.; Seo, J. I.; Hunziker, Ch.; Schneider, A.; Yun, H.; Lee, Y. S.; Günter, P. *Adv. Funct. Mater.* **2008**, *18*, 3242.
(16) For example, Rainbow Photonics AG. www.rainbowphotonics.com (accessed December 21, 2010).
(17) (a) Jazbinsek, M.; Mutter, L.; Günter, P. P. *IEEE J. Sel. Top. Quantum Electron.* **2008**, *14*, 1298. (b) Hunziker, Ch.; Kwon, S. J.; Figi, H.; Juvalta, F.; Kwon, O. P.; Jazbinsek, M.; Günter, P. *J. Opt. Soc. Am. B* **2008**, *25*, 1678.
(18) (a) Suizu, K.; Miyamoto, K.; Yamashita, T.; Ito, H. *Opt. Lett.* **2007**, *32*, 2885. (b) Schneider, A.; Stillhart, M.; Günter, P. *Opt. Express* **2006**, *14*, 5376. (c) Stillhart, M.; Schneider, A.; Günter, P. *J. Opt. Soc. Am. B* **2008**, *25*, 1914.
(19) Brunner, F. D. J.; Kwon, O. P.; Kwon, S. J.; Jazbinsek, M.; Schneider, A.; Günter, P. *Opt. Express* **2008**, *16*, 16496.
(20) Kwon, S. J.; Jazbinsek, M.; Kwon, O. P.; Günter, P. *Cryst. Growth Des.* **2010**, *10*, 1552.
(21) Kwon, O. P.; Jazbinsek, M.; Yun, H.; Seo, J. I.; Seo, J. Y.; Kwon, S. J.; Lee, Y. S.; Günter, P. *CrystEngComm* **2009**, *11*, 1541.
(22) Kwon, S. J.; Kwon, O. P.; Seo, J. I.; Jazbinsek, M.; Mutter, L.; Gramlich, V.; Lee, Y. S.; Yun, H.; Günter, P. *J. Phys. Chem. C* **2008**, *112*, 7846.

J = 18 Hz, −CH=CH-), 7.46−7.49 (2H, d, J = 8.7 Hz, Ar−H). Elemental analysis for $C_{18}H_{16}N_2O$: (%) calcd. C 78.24, H 5.84, N 10.1, O 5.79; found: C 78.29, H 5.82, N 10.2, O 5.77.

X-ray Crystallographic Data. *OH2-(I) Crystal.* $C_{18}H_{16}N_2O$, M_r = 276.34, monoclinic, space group *Cc*, a = 10.9906(10) Å, b = 13.9947(10) Å, c = 9.9856(9) Å, β = 93.944(3)°, V = 1532.3(2) Å^3, Z = 4, T = 290(1) K.

OH2-(II) Crystal. $C_{18}H_{16}N_2O$: M_r = 276.34, monoclinic, space group $P2_1/n$, a = 9.2223(4) Å, b = 13.3508(6) Å, c = 12.1780(7) Å, β = 94.461 (2)°, V = 1494.87(12) Å^3, Z = 4, T = 290(1) K (see the Supporting Information).

Further details of the crystal structure investigation(s) may be obtained from the Cambridge Crystallographic Data Centre (CCDC, 12 Union Road, Cambridge CB2 1EZ (UK); tel.: (+44)1223−336−408, fax: (+44)1223−336−033, e-mail: deposit@ccdc.cam.ac.uk) on quoting the depository number CCDC-682356 for OH2-(I) and CCDC-785661 for OH2-(II).

Results and Discussion

Design of Phenolic Polyene Crystals. We have chosen configurationally locked polyene (CLP) molecules[13,14] with phenolic electron donor groups due to their tendency of acentric molecular ordering in the crystalline state and high thermal stability.[15] The chemical structures of the phenolic CLP chromophores are shown in Figure 1. In both previously investigated OH1 and OH3 crystals, the main supramolecular interactions are strong head-to-tail hydrogen bonds of −OH...NC− groups, which build polymer-like polar chains in the crystalline solid.[15,21] The π-conjugated part of the chemical structure of these chromophores is equivalent and the difference is in the presence of methyl groups on the non-π-conjugated part in the cyclohexene ring. The crystal structure of OH1 and OH3 has been shown to strongly depend on the existence of the axial methyl group. The axial methyl group in OH1 molecule, which has two methyl groups, forms weak hydrogen bonds −CH...NC− in the crystal structure, and leads to a crosslike packing of the polar molecular chains, in contrast to the perfectly parallel packing of the polar chains of OH3 molecules without methyl groups.[21] Resulting from the small difference in the chemical structure, the order parameter, which is essential for the macroscopic second-order nonlinearity, is considerably higher in OH3 compared to OH1.[15,21] However, although OH3 crystals show an almost perfect molecular ordering in the crystalline state, due to a low solubility and a very poor crystal growth, OH3 bulk crystals suitable for optical experiments could not be grown. On the other hand, large bulk OH1 crystals with size of 18 × 17 × 4 mm^3 were grown by a relatively simple solution growth method.[20] To achieve optimal physical properties and crystal characteristics by combining advantages of OH1 and OH3, we designed a new phenolic CLP chromophore without changing the main supramolecular interaction sites (i.e.,−OH and −CN groups), by introducing only non-axial (i.e., equatorial) methyl substituent[22] on the cyclohexene ring. It is therefore expected that this small chemical modification can change the weak intermolecular hydrogen bonds in the crystalline packing compared to OH1, potentially keeping the optimal structure achieved in the OH3 crystal structure, but the other physical properties can be improved compared to OH3 crystals.

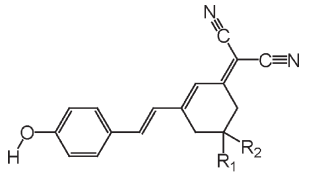

R_1	R_2	Abbr.
CH_3	CH_3	OH1
CH_3	H	OH2
H	H	OH3

Figure 1. The chemical structure of the investigated CLP chromophores with phenolic electron and hydrogen bond donor.

Single Crystal Structures. Single crystals of OH2 crystals were grown from methanol or acetonitrile solution by the slow evaporation method. The single crystal structures of OH2 crystals were determined by X-ray diffraction. We observed two polymorphs of OH2 crystals: OH2-(I) phase with acentric monoclinic space group symmetry *Cc* (point group *m*) when grown from methanol and OH2-(II) with centrosymmetric monoclinic space group symmetry $P2_1/n$ (point group $2/m$) when grown from acetonitrile (see Table 1). The OH1 and OH3 crystals have acentric orthorhombic space group symmetry $Pna2_1$ (point group *mm*2) and monoclinic with space group symmetry *Cc* (point group *m*), respectively; for both OH1 and OH3 no polymorphs were observed. The crystal packing diagrams of

Table 1. Summary of Crystallographic Data for the Phenolic Polyene Crystals

	OH1 [15]	OH2-(I)	OH2-(II)	OH3 [21]
formula	$C_{19}H_{18}N_2O$	$C_{18}H_{16}N_2O$	$C_{18}H_{16}N_2O$	$C_{17}H_{14}N_2O$
formula weight	290.37	276.34	276.34	262.31
crystal system	orthorhombic	monoclinic	monoclinic	monoclinic
space group	$Pna2_1$	*Cc*	$P2_1/n$	*Cc*
a (Å)	15.4408(6)	10.9906(10)	9.2223(4)	10.9927(8)
b (Å)	10.9939(3)	13.9947(10)	13.3508(6)	12.5852(9)
c (Å)	9.5709(3)	9.9856(9)	12.1780(7)	10.1326(6)
α (deg)	90	90	90	90
β (deg)	90	93.944(3)	94.4610(16)	94.3637(19)
γ (deg)	90	90	90	90
V (Å^3)	1624.70(9)	1532.3(2)	1494.87(12)	1397.73(16)
Z	4	4	4	4
volumer (Å^3/molecule)	406.2	383.1	373.7	349.4
hydrogen bond length (O···N)	2.96	2.87	2.90	2.81
CCDC deposit number	CCDC-672263	CCDC-682356	CCDC-785661	CCDC-682357

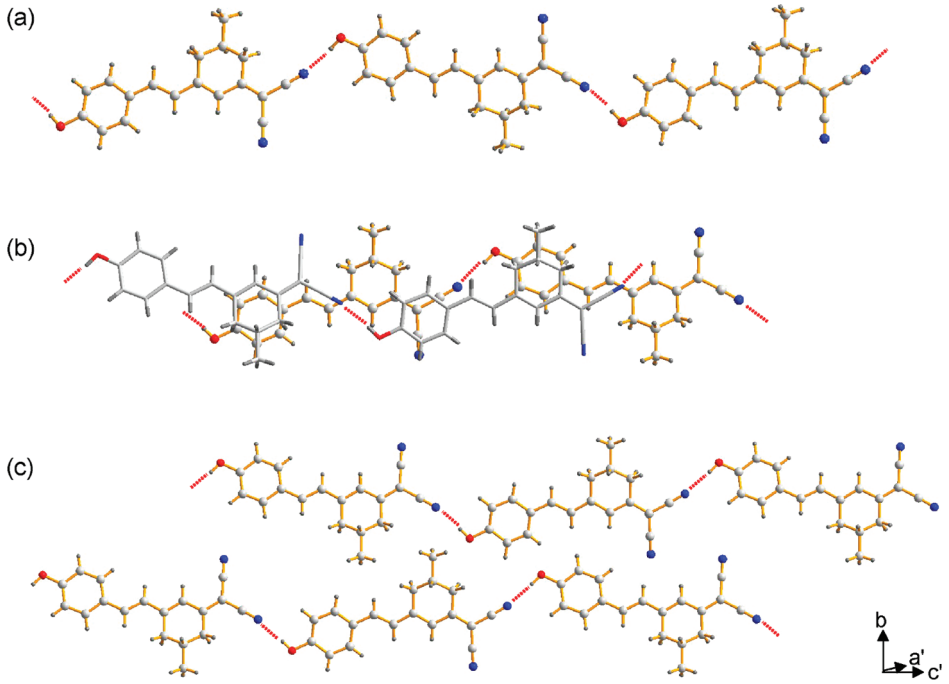

Figure 2. (a) Crystal packing diagram of acentric OH2-(I) crystals: OH2 molecules are linked with hydrogen bonds of C≡N···H−O with N···H distances of about 2.06 Å, which are indicated by dotted lines. (a) Top view of an acentric chain, (b) top view of a stack of two acentric chains, and (c) top view of parallel two acentric chains; a' and c' are the projections of the a and c crystallographic axes to the image plane.

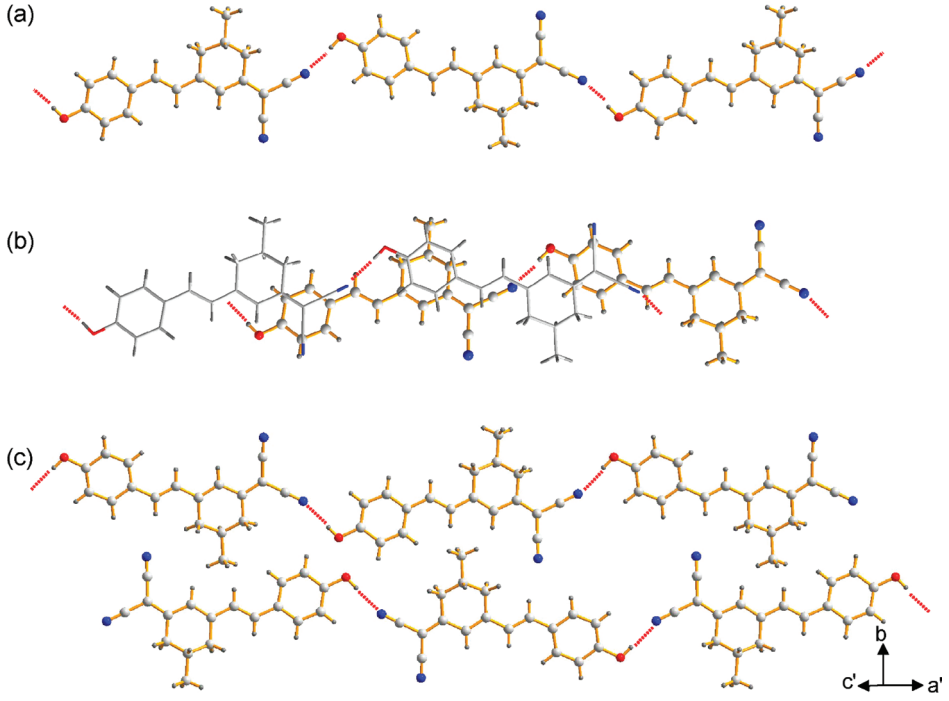

Figure 3. Crystal packing diagram of centrosymmetric OH2-(II) crystals: OH2 molecules are linked with hydrogen bonds of C≡N···H−O with N···H distances of about 2.09 Å, which are indicated by dotted lines. (a) Top view of an acentric chain, (b) top view of a stack of two acentric chains, and (c) top view of two parallel acentric chains; a' and c' are the projections of the a and c crystallographic axes to the image plane.

OH2 crystals are shown in Figure 2 for acentric OH2-(I) phase and Figure 3 for OH2-(II) phase.

As in OH1 and OH3 crystals, the main supramolecular interactions of both OH2-(I) and OH2-(II) phases are strong head-to-tail hydrogen bonds of C≡N···H−O with N···H distances of about 2.06 Å. Therefore, as expected the small modification by introducing one methyl substituent does not affect the main supramolecular interactions. In both OH2-(I) and OH2-(II) phases, OH2 molecules form acentric polar chains linked between each ends of the molecules (see Figures 2a and 3a), and the acentric chains are acentrically stacked up one by one (see Figures 2b and 3b). The difference between OH2-(I) and OH2-(II) phases results from minor intermolecular interactions and not from the

main intermolecular interactions: As shown in Figures 2c and 3c, the adjacent acentric chains are aligned parallel in OH2-(I) and antiparallel in OH2-(II).

Due to the very good acentric molecular ordering of the OH2-(I) phase, which is promising for second-order nonlinear optical applications, these crystals have been investigated in more detail. OH2-(I) crystals having one methyl group in the cyclohexene ring of the molecules have an isomorphic structure with OH3 crystals without the methyl group, which is different as for OH1 crystals with two methyl groups. The reason is related to the existence of the axial methyl group in the cyclohexene ring: the axial methyl group in OH1 crystals forms interchain weak hydrogen bonds that do not exist in OH3.[21] The methyl group on the cyclohexene ring of OH2 molecules has an equatorial position in the crystalline state. This results in an equivalent packing of molecules in OH2-(I) and OH3 crystals.

Although the crystal structures of OH2-(I) and OH3 crystals are similar, a different number of the methyl groups in the non-π-conjugated part of the molecules influences the details of molecular ordering. Decreasing the number of methyl groups results in decreasing the length of the main supramolecular hydrogen bonds of C≡N···H−O with a O···N distance of about 2.96 Å, 2.87 Å, and 2.81 Å for OH1, OH2-(I), and OH3 respectively (see Table 1). In addition, the volume occupied by one molecule also decreases (see Table 1), which increases the number density of chromophores in the crystalline state, as listed in Table 2. This may change the physical properties, as discussed in the following sections.

Molecular and Macroscopic Nonlinearity with Optimal Molecular Packing. The results of the physical characteristics, including the thermal properties, absorption properties, macroscopic nonlinearity, and crystal properties of phenolic CLP crystals, are summarized in Table 2. Since the chemical modification is in the non-π-conjugated part of the phenolic CLP chromophores, OH2 molecule is expected to have similar electronic properties as OH1 and OH3 molecules, which affect the UV−vis absorption in solution and the microscopic molecular nonlinearity. All phenolic CLP molecules in methanol exhibit a similar wavelength of maximum absorption λ_{max} of about 424 nm, confirming that the electronic polarizability properties are similar. In order to evaluate the microscopic nonlinearity, the maximal first-order hyperpolarizability β_{max} was calculated by quantum chemical calculations[22] using the hybrid functional B3LYP[23] with the 6-311+G(d) basis set. The experimental (EXP) molecules occurring in the OH2-(I) phase, determined by the X-ray diffraction analysis, were analyzed by the finite field (FF) method. The results of the quantum chemical calculations are listed in Table 2 with more details in the Supporting Information. As expected, the maximal first-order hyperpolarizability β_{max} (the hyperpolarizability component along the main charge-transfer direction) of OH2 chromophore is similar as for the other two chromophores (see Table 2).

Table 2. Physical and Structural Data of the Investigated Phenolic Polyene Derivatives[c]

	λ_{max} (nm)	T_m/T_i(°C)	solubility @ 35 °C (g/100 g methanol)	$\beta_{max}{}^a$ (10^{-30} esu)	$\beta_{iii}^{eff\,a}$ (10^{-30} esu)	$\beta_{max}{}^b$ (10^{-30} esu)	$\beta_{max}(D)^b$ (10^{-30} esu)	$\beta_{iii}^{eff}(D)^b$ (10^{-30} esu)	order parameter $\cos^3(\theta_p)$	number density (molecule/10^3 Å^3)	powder SHG
OH1	425	212/325	3.07	93	63	85	116	86	0.69	2.46	1
OH2-(I)	424	242/326	0.88	90	82	83	125	125	0.92	2.61	1–2
OH3	424	283/310	0.45	86	79	80	121	121	0.93	2.86	1

[a] B3LYP/6-311+G(d). [b] B3LYP/6-31G(d). [c] The maximal first-order hyperpolarizability β_{max} determined by quantum chemical calculations using B3LYP/6-311+G* or B3LYP/6-31G* and considering EXP molecules (conformation from the crystal structure). The diagonal component of the effective hyperpolarizability tensor $\beta_{ijk}^{eff} \propto \chi_{ijk}^{(2)}$ along the polar axis ($\beta_{333}{}^{eff}$ for OH1; $\beta_{111}{}^{eff}$ for OH2 and OH3) calculated from the hyperpolarizability tensor components β_{mnp} by considering the orientation of the chromophores in the crystallographic system. Powder SHG efficiency was measured at a fundamental wavelength of 1.9 μm relative to OH1 powder. λ_{max}: the wavelength of the maximum absorption in methanol solution, T_i: the thermal weight-loss temperature, T_m: the melting temperature, (D): results considering dimers (see text).

(23) (a) Becke, A. D. *J. Chem. Phys.* **1993**, *98*, 5648. (b) Perdew, J. P. *Phys. Rev. B* **1986**, *33*, 8822.

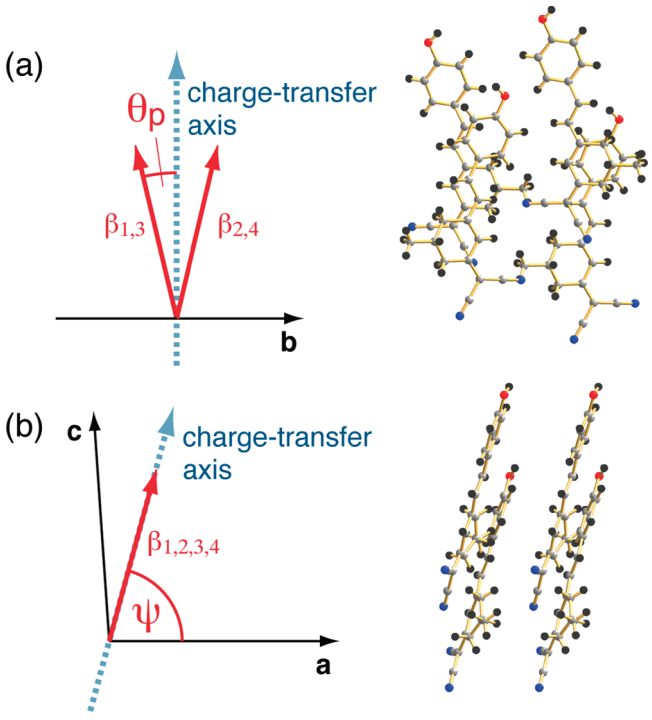

Figure 4. Crystal packing diagram of the acentric OH2-(I) crystalline phase projected to the plane containing the charge transfer axis and the *b*-axis (a) and to the *ac* plane (b). The solid vectors present the directions of the maximum first hyperpolarizability β_{max} of four OH2 molecules in the unit cell as determined by finite-field (FF) calculations, while the dotted vectors present the direction of the effective charge transfer axis of the crystal. The angle between the main charge-transfer axis of the crystal, which is in the *ac* plane (ψ = 75°), and the charge-transfer axes of the molecules is θ_p = 13.3°.

From quantum chemical calculations, taking into account all tensor component of the zero-frequency hyperpolarizability tensor β_{ijk}, we calculated the main charge-transfer directions of acentric chains in the crystallographic system,[22] which are illustrated in Figure 4. As a consequence of the almost parallel molecular packing of the chromophores,[21] OH2-(I) crystals exhibit only a small angle between the main charge-transfer direction of the molecules and the polar axis of the crystals $\theta_p \approx 13°$, which leads to a large order parameter of the crystal, $\cos^3 \theta_p$ = 0.93, similar as in the isomorphic OH3 crystals, while OH1 crystals possess a lower order parameter $\cos^3 \theta_p$ = 0.69. OH2-(I) crystals are therefore expected to exhibit a large diagonal macroscopic second-order susceptibility element.

The macroscopic nonlinearity of the newly synthesized OH2 crystals has been estimated by quantum chemical calculations and measured with the Kurtz and Perry powder test.[24] The components of the effective hyperpolarizability tensor β^{eff}_{ijk} in the crystal have been calculated from the hyperpolarizability tensor components β_{mnp} of the molecules by using the well-known oriented-gas model[7c]

$$\beta^{eff}_{ijk} = \frac{1}{n(g)} \sum_{s}^{n(g)} \sum_{mnp}^{3} \cos(\theta^{s}_{im}) \cos(\theta^{s}_{jn}) \cos(\theta^{s}_{kp}) \beta_{mnp} \quad (1)$$

where $n(g)$ is the number of equivalent positions in the unit cell, s denotes a site in the unit cell, and θ^{s}_{im} is the angle between the Cartesian axis i and the molecular axis m. The main component of the effective hyperpolarizability tensor is for all OH crystals the diagonal component along the polar axis and is listed in Table 2; more detailed results can be found in Table S2 of the Supporting Information. OH2-(I) crystals with an optimal molecular packing show an about 30% larger diagonal component of the effective hyperpolarizability tensor β^{eff}_{iii} than OH1 crystals.

Precise experimental determination of the nonlinear optical susceptibility elements require several crystals cut and polished along different crystallographic directions as well as precise determination of the refractive indices along these directions, which is beyond the scope of this work. Such characterization has been previously done for OH1 crystals.[17b] In view of the similar molecular properties of OH1 and OH2 and the known chromophore packing, we can expect that the macroscopic nonlinear susceptibility tensor elements $\chi^{(2)}_{ijk}$ follow the trend of the calculated β^{eff}_{ijk} elements. In the oriented-gas model, the macroscopic susceptibility tensor elements are related to the effective hyperpolarizabilities β^{eff}_{ijk} as

$$\chi^{(2)}_{ijk} = NF_{ijk}\beta^{eff}_{ijk} \quad (2)$$

where N is the number density of the molecules, and F_{ijk} is the correction factor due to intermolecular interactions. Most often, for F_{ijk} the local-field corrections due to the dielectric environment are considered, which gives in the case of second-harmonic generation the following expression

$$F^{SHG}_{ijk} = \frac{n_i^2(2\omega)+2}{3} \cdot \frac{n_j^2(\omega)+2}{3} \cdot \frac{n_k^2(\omega)+2}{3} \quad (3)$$

where $n_i(\omega)$ is the refractive index along the axis i at the frequency ω. In first approximation, we can neglect the difference between the local-field factor F of OH2 compared to OH1 for the diagonal $\chi^{(2)}$ coefficient. In fact, because of the better alignment and similar molecular polarizabilities of these molecules (see the Supporting Information), the refractive index of OH2 along the polar axis should be higher as for OH1, which will lead to an additional enhancement of the diagonal $\chi^{(2)}$ element along this axis. Only considering the number density of the molecules and the effective hyperpolarizability of the crystal, the diagonal $\chi^{(2)}$ coefficient is expected to be 40% larger in OH2 compared to OH1 crystals. In the same way, the diagonal electro-optic figure of merit n^3r, which is related to the $\chi^{(2)}$ coefficient approximately as $n^3r \sim \chi^{(2)}/n$, can be expected at least 40% higher as in OH1 crystals. Note that the electro-optic figure of merit n^3r = 530 pm/V at 1319 nm of OH1 crystals is already very high, very similar as in DAST crystals, which presents the highest electro-optic figures of merit measured to date in organic crystals.[17]

A simple way to confirm the validity of the above estimations is by measuring the second-harmonic generation efficiency of the crystalline powder under nonresonant conditions. The macroscopically observed powder-test efficiency is proportional to the square of the chromophore density N and the squared β^{eff}_{ijk} components, spatially

(24) Kurtz, K.; Perry, T. T. *J. Appl. Phys.* **1968**, *39*, 3798.

averaged considering the corresponding point group symmetry.[24] The calculated $N^2\langle(\beta^{eff})^2\rangle$ is by a factor of 1.5 and 1.7 respectively larger for OH2 and OH3 compared to OH1, which is a result of the high order parameter and more compact chromophore packing.

The Kurtz and Perry powder test experiment[24] was performed at a fundamental wavelength of 1.9 μm by measuring the transmitted nonresonant second harmonic generation (SHG) efficiency of ungraded powder samples. While the SHG efficiency of OH3 powder was similar as for OH1 powder, OH2-(I) powder exhibited a powder SHG efficiency of 1.5 ± 0.5 of OH1, based on several powder SHG experiments with differently prepared powders for these phenolic CLP compounds. This result is according to the theoretical expectations for OH1 and OH2. For OH3 the lower efficiency may be the consequence of the particle size as well as some other effects like intermolecular interactions, which may influence the hyperpolarizability of a single molecule in the solid state.

Head-to-Tail Hydrogen Bonds and First Hyperpolarizability. In order to further understand the reasons for the different powder SHG efficiency of OH1, OH2, and OH3 crystals, we performed quantum chemical calculations by using the finite field (FF) methods considering: 1) the influence of the main hydrogen bonds on the molecular nonlinearity in the crystalline state and 2) the influence of the strength of these bonds. To investigate the influence of forming the hydrogen bonds on the molecular nonlinearity, we first calculated the maximal nonresonant first-order hyperpolarizability β_{max} of a single EXP molecule, and second the first hyperpolarizability β_{max}(D) of an EXP molecule in a dimer containing the main hydrogen bond in the crystals using B3LYP/6-31G* (see the inset of Figure 5). The results are listed in Table 2 and Table S3. The maximal first-order hyperpolarizability β_{max}(D) of a molecule in such a dimer is enhanced compared to a single EXP molecule, confirming that head-to-tail hydrogen bonds between the chromophores may enhance the molecular nonlinearity.[25] Moreover, the enhancement of the maximal first-order hyperpolarizability of a chromophore is different in phenolic CLP crystals: 1.52 times for OH2 and OH3 and 1.36 times for OH1. Therefore, the diagonal component of the effective hyperpolarizability tensor β_{iii}^{eff} (D) considering the enhancement of the maximal first-order hyperpolarizability in dimers is also enhanced and OH2 crystals exhibit the largest diagonal effective hyperpolarizability tensor element β_{iii}^{eff} (D), almost 50% larger as in OH1 crystals. Note that this is only an example estimation considering the main interacting molecule by the strongest hydrogen bond and only on one side of the molecule, still it shows that the influence of the intermolecular hydrogen bonds on the hyperpolarizability of a single molecule in the solid state may be huge. On the other hand, we did not observe considerable differences between the OH2 and OH3 dimers, even when considering other dimers (other neighboring molecules), which influence the first hyperpolarizability to a smaller extent.

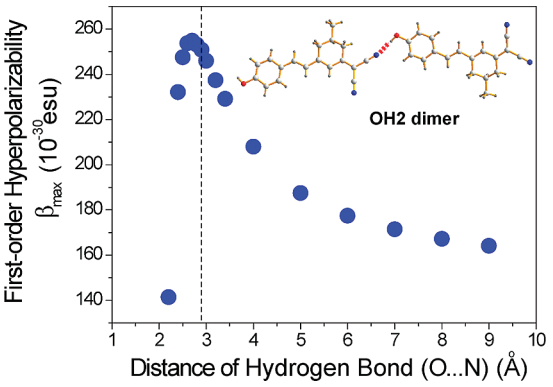

Figure 5. Influence of the strength of the −OH···NC- hydrogen bonds on the molecular nonlinearity. The maximal first-order hyperpolarizability β_{max} of dimers was calculated with finite-field (FF) method using B3LYP/6-31G(d). The initial dimer structure is from the OH2-(I) crystal structure, which is indicated by the vertical dotted line.

Considering the different length of the strong hydrogen bonds of OH···NC forming main supramolecular interactions of phenolic CLP crystals (O···N distance of about 2.96 Å, 2.87 Å, and 2.81 Å for OH1, OH2-(I), and OH3, respectively), we also investigated the influence of the strength of these hydrogen bonds on the molecular nonlinearity. The maximal first-order hyperpolarizability β_{max} of dimers in OH2-(I) crystals was calculated with various OH···NC hydrogen-bond distances. For this calculation, all atoms were kept in the position as determined from the X-ray diffraction analysis, where the hydrogen-atom positions were evaluated by using the riding method. As shown in Figure 5, the maximal first-order hyperpolarizability β_{max} of dimers is strongly dependent on the strength of this hydrogen bond with large variations, changing the hyperpolarizability values of a single molecule by a factor of 2. The length of the hydrogen bonds of all phenolic CLP crystals is near the optimum of the intermolecularly enhanced first-order hyperpolarizabilities β_{max}.

Tailored Physical Properties and Crystal Growth. Thermal properties and solubility are important parameters for a reliable crystal growth by melt, vapor, and solution growth methods.[1b] Previously developed OH3 crystals with optimal molecular ordering exhibit poor crystal growth, and we could not obtain bulk single crystals suitable for optical experiments.[21] On the other hand, OH1 crystals show excellent crystal growth characteristics.[15,20] The OH2 crystals also with optimal molecular ordering exhibit physical properties between OH1 and OH3 crystals (see Table 2). Thermal properties were investigated by thermogravimetric analysis (TGA) and differential scanning calorimetry (DSC) (10 °C/min heating rate). All phenolic CLP crystals exhibit a high thermal stability with the thermal weight-loss temperature T_i > 310 °C. The OH3 crystals reveal a small difference between the thermal weight-loss temperature T_i and the melting temperature T_m (T_i = 310 °C, T_m = 283 °C, $\Delta T = T_i - T_m$ = 23 °C), which is practically already limiting

(25) (a) Datta, A.; Pati, S. K. *Chem. Soc. Rev.* **2006**, *35*, 1305. (b) Castet, F.; Champagne, B. *J. Phys Chem. A* **2001**, *105*, 1366. (c) Fujiwara, M.; Yanagi, K.; Maruyama, M.; Sugisaki, M.; Kuroyanagi, K.; Takahashi, H.; Aoshima, S.; Tsuchiya, Y.; Gall, A.; Hashimoto, H. *Jpn. J. Appl. Phys.* **2006**, *45*, 8676. (d) Kwon, O. P.; Jazbinsek, M.; Yun, H.; Seo, J. I.; Kim, E. M.; Lee, Y. S.; Günter, P. *Cryst. Growth Des.* **2008**, *8*, 4021.

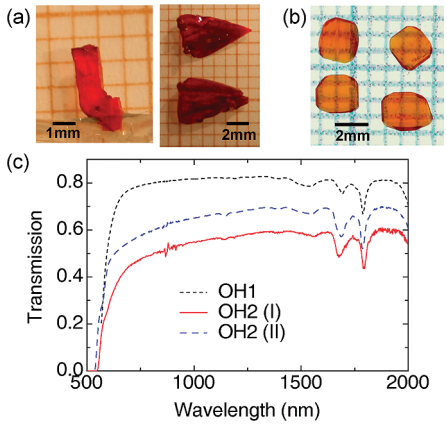

Figure 6. Bulk OH2 crystals grown by slow evaporation method: (a) acentric OH2-(I) from methanol solution and (b) centrosymmetric OH2-(II) from acetonitrile solution. Transmission spectra of a polished 0.3-mm thick OH1 (black dotted line), an unpolished 0.25-mm thick OH2(I) crystal (red solid line), and an unpolished 0.3-mm thick OH2(II) crystal (blue dashed line) using unpolarized light.

the potential for the melt-based crystal growth. OH2-(I) crystals show a large difference between $T_i = 326$ °C and $T_m = 242$ °C ($\Delta T = T_i - T_m = 84$ °C), which is an advantage for applying melt and vapor growth techniques.

One more methyl group on the flexible aliphatic part in OH2 chromorphore compared to OH3 chromophore affects considerably the solubility. The solubility of OH2 is about 0.88 g/100 g methanol and of OH3 0.45 g/100 g methanol at 35 °C. OH2 exhibits almost twice the solubility of OH3 in methanol, which is an advantage for solution-based crystal growth. As a consequence of the improved solubility, bulk single OH2 crystals were obtained by the slow evaporation method in methanol solution for OH2-(I) and acetonitrile solutions for OH2-(II) as shown in Figure 6a,b. As grown acentric OH2-(I) crystals obtained like this are optical quality single crystals with up to $6 \times 4 \times 1$ mm in size. Figure 6c shows transmission spectra of an unpolished 0.25-mm thick OH2-(I) crystal, an unpolished 0.3-mm thick OH2-(II) crystal, and a polished 0.3-mm thick OH1 crystal using unpolarized light. The unpolished OH2 crystals exhibit a good optical quality without too much scattering and the transmission is similar as for polished OH1 crystals. All three OH crystals in Figure 6c exhibit a large transparency range from 700 to 1400 nm.

Conclusions

We have investigated the nonlinear optical organic phenolic CLP chromophores with a different design of the non-π-conjugated part to achieve desired crystalline packing and to tailor their physical properties. Newly designed phenolic OH2 crystals containing different substituents in the non-π-conjugated part in the cyclohexene ring maintain the main supramolecular interactions of the previously studied OH1 and OH3 crystals but result in a more optimal packing compared to OH1 crystals and better crystal processing properties compared to OH3 crystals. Depending on the solvent, OH2 crystals with two polymorphic forms have been obtained, with the acentric monoclinic space-group symmetry *Cc* (OH2-(I)) and the centrosymmetric monoclinic space-group symmetry $P2_1/n$ (OH2-(II)). OH2-(I) crystals exhibit a large macroscopic nonlinearity with up to twice the second harmonic generation efficiency of OH1 crystals, which is attributed to the molecular alignment with a high order parameter $\cos^3 \theta_p = 0.92$. This, together with the results of the theoretical quantum chemical analysis, shows that the diagonal electro-optic figures of merit of OH2 can be considerably (~40%) increased compared to the state-of-the-art values in OH1 and DAST crystals. Moreover, OH2-(I) crystals in contrast to OH3 crystals show a good crystal growth with about twice the solubility in methanol, and therefore OH2 bulk crystals suitable for optical investigations have been grown, which was not possible with isomorphous OH3 crystals. Therefore, OH2 crystals are very promising materials for practical applications, having not only a large macroscopic nonlinearity with optimal molecular ordering but also good crystal characteristics including the crystal growth, solubility, and high thermal stability.

Acknowledgment. This work has been supported by Basic Science Research Program (2010-0009541) and Priority Research Centers Program (2010-0028294) through the National Research Foundation of Korea (NRF) funded by the Ministry of Education, Science and Technology and by the Swiss National Science Foundation (200020-119958). The research at KAIST was supported by Midcarrier Research Program (2009-0084918) and CMD (2010-001632).

Supporting Information Available: Details of X-ray crystallographic data and computational calculations. This material is available free of charge via the Internet at http://pubs.acs.org.